International Journal of Engineering

Journal Homepage: www.ije.ir

Control of Steel Detachment and Metal Flow on Aluminum-steel Friction Stir Welding of Thin Joints

E. A. Torres[a], J. Graciano-Uribe[b], T. F. A. Santos[c]

[a] *Department of Mechanical Engineering, Research Group - GEA, Universidad de Antioquia, Medellín, Colombia*
[b] *Department of Mechatronics Engineering, Research Group - MATyER, Instituto Tecnológico Metropolitano, Medellín, Colombia*
[c] *Department of Mechanical Engineering, Universidade Federal de Pernambuco, Research group- SOLDAMAT, Recife, Brazil*

PAPER INFO

Paper history:
Received 10 November 2019
Received in revised form 23 December 2019
Accepted 04 January 2020

Keywords:
Dissimilar Joints
Offset Effect
Steel Fragments Formation
Restriction to Metal Flow

ABSTRACT

In the last thirty years, the friction stir welding (FSW) process has achieved significant importance due to the satisfactory results derived from severe deformation and low heat input during the welded joint production. These elements have been considered to implement the FSW in different welded systems, including aluminum-steel joints. In these dissimilar joints, the main interest was to obtain a welded joint with acceptable mechanical behavior. Some papers recently focused on understanding dissimilar joints process, mainly on the metal flow and its response to corrosion. However, in Al-steel joints, the presence of steel particles in the nugget zone is routine, it alters both the mechanical and chemical behavior of welded joints. Thus, this work aims to evaluate the mechanisms that govern these particles' generation, the effect of offset on their formation, and proposing the material flow behavior, using the detached fragments as tracers. It was established that the offset controls the metal's fluidity, which allows the accumulation of steel fragments on the advanced side, and reducing its quantity, due to the decrease of irregularities in the Al-steel interface. Likewise, the metal flow was observed on the retreating side, with that mentioned in aluminum joints. In contrast, on the advanced side, there is a shear action, push down, and lateral movement towards the retreating side, driven by the high forging strength of the metal and the restriction imposed by the steel and the backing.

***doi**: 10.5829/ije.2021.34.04a.29*

NOMENCLATURE

FSW	Friction stir welding	F_r	Rotational force (N)
IMC	Intermetallic compounds	P_E	Effective depth
O_r	Real offset (mm)	RS	Retreating side
O_T	Tangent offset (mm)	AS	Advancing side
P_T	Tool penetration (mm)	**Greek Symbols**	
OM	Optical microscopy	ω	Rotation speed (rpm)
SZ	Stir zone	υ	Welding speed (mm/min)
TMAZ	Thermo-mechanically affected zone	δ	slip/stick factor (mm/rev)
F_t	Travel force (N)	λ	spacing between bands (mm)

1. INTRODUCTION

Energy consumption is a notable factor in the design of new transport systems. Therefore, the reduction of vehicle weight, without compromising the integrity of the structure, is the target of many studies [1], with a focus on the automotive, [2, 3], naval [4], aeronautics [5] and aerospace [6, 7] industries. In this sense, different methodologies have emerged and continue to be evaluated. One of these is the Friction Stir Welding (FSW) process, developed by TWI in 1991 [8], which is a technique for joining and processing materials that arose from the concept of conventional friction welding. FSW uses a tool to produce heat while generating severe plastic deformation, resulting in a mechanical/metallurgical mixture of the plasticized

*Corresponding Author Email: eandres.torres@udea.edu.co (E. A. Torres)

Please cite this article as: E. A. Torres, J. Graciano-Uribe, T. F. A. Santos, Control of Steel Detachment and Metal Flow on Aluminum-steel Friction Stir Welding of Thin Joints, International Journal of Engineering, Transactions A: Basics Vol. 34, No. 04, (2021) 1024-1034

metal [9], [10]. The tool, formed by a pin and a shoulder, has two main functions: locally heat the workpiece and stir the material to obtain the welded joint. The combined movement of rotation and translation in the tool generates relative displacement due to different speeds in both side of the tool, allowing a complex flow of metal in the plasticized zone and, consequently, consolidating a welded joint [11, 12].

Plasticized metal is limited by the tool, solid metal, and backing plate, which forces it to flow around the tool, forming the joint [13]. The flow complexity is accentuated by the tool's geometric features, such as threads and flutes, designed to drive the material and to promote adequate material mixing [14, 15]. Due to the complexity of the metal flow, different types of defects can be found, which include surface defects, voids, and lack-of-fill. The latter two are the result of low plasticity of the material and loss of filling capacity. In this sense, it was determined that the pitch (υ/ω) is an essential variable for controlling voids and kissing bonds [16].

The welding of dissimilar joints [17, 18] was approached considering three different systems: i) dissimilar joints of low melting metals, ii) the joining of hard metals, and iii) the joining of metals with different mechanical properties. The welding of systems composed of metals with very different physical properties has limitations due to the multiple challenges. The main ones are the difference in the melting temperature and mechanical strength. The FSW of dissimilar metals is different from the welding of the same metal systems by forming a more heterogeneous flow of metal [19]. Also, few references to the metal flow in the FSW of Al-steel joints make it difficult to understand and control the generation of defects.

The first experiments with welding dissimilar joints using FSW ended with developing new welding parameters, based on the flow of the plasticized material and the asymmetry of heat generation in the joint [20], which are the joint configuration and the position of the tool. The joint configuration determines how the plates should be positioned considering the advancing and retreating sides. The joint configuration for welding metals with different melting temperatures places the hardest metal on the advanced region, which is the side where the temperature generated by friction is higher [21]. The parameter that determines the position of the tool is called offset. Therefore, the offset defines the position of the tangent of the pin to the joint line, being positive when it enters steel and negative when the pin is entirely in aluminum [22, 23]. From these recommendations, Yasui [24] obtained welded joints AA6063-steel, where he related the effect of υ and ω with the plastic flow and the formation of defects, similar to what happened when welding joints of the same metal.

In addition to the complex flow of metal, the detachment of steel is usual in this type of welded joint. The majority of papers on the subject mention such fragments without going into greater detail [25]. Several works point to the formation of intermetallic compounds (IMC) around steel particles [26], while others evaluate their effect on the response to corrosion of the joint [27], being that the increment in the number of fragments significantly increases the corrosion rate [23-28]. It should be noted that different strategies have been presented to investigate the flow of material during FSW, such as insertion of markers, three-dimensional analysis using X-ray tomography or X-ray radiography in situ, use of different materials, the use of plasticine, and applied freezing after the pin breaks [29]. In one of the first works, Colligan [30] used steel markers to determine the material flow in aluminum joints. Consequently, the steel fragments detached during the FSW of Al-steel joints can be used as markers to follow the plasticized metal flow in the nugget zone.

Therefore, it is essential to understand the effect of welding parameters on the mechanisms that produce these particles and the strategies to control their formation. Furthermore, it is crucial to understand the plasticized metal flow since the detached particles' position and characteristics depend on it. This manuscript assesses the effect of offset on the formation, size, and distribution of the steel particles detached and deposited in the mixing zone. The paper also presents a proposal about the offset's influence in the aluminum plasticization process and the metal's flow in thin aluminum-steel joints welded by FSW. The authors would like to highlight the major concern about joining aluminum and steel are the variety of deleterious intermetallic compounds in the fusion zone, in case of fusion welding processes and the nugget zone when friction stir welding is used. The ability to achieve the pursued challenge, which is Al-steel joining, is connected to a better understanding and controlling the nugget zone precipitation.

2. MATERIALS AND METHODS

The materials used were aluminum alloy plates 6063-T5 and AISI SAE 1020 steel, both with dimensions of 500 × 85 × 2.0 mm. Welding was performed using a dedicated FSW machine from Transformation Technologies Incorporated (TTI), model RM-2. The machine has complete control of the welding parameters (rotation and welding speed), even with penetration of the tool controlled by position or axial load. In addition, the device has torque, liquid cooled tool holder, and wireless temperature acquisition system required for continuous real time temperature data control. A metal matrix and ceramic reinforcement tool of tungsten carbide (WC-14Co) were used, with shoulder and pin of 25 and 5.7 mm in diameter, respectively, and a pin length of 1.35 mm.

Figure 1a shows the configuration of the joint. The positioning of tool was done using two criteria: the tangent offset (O_T) and the tool real offset (O_R). The first considers the distance between the pin and the joint line's tangent, while the second holds the radius of the pin (5.7 mm) plus the displacement of the tangent (Figure 1b).

The joints were produced using ceramic backing [31]; however, to demonstrate the complete material flow, joints were made using a 5052-aluminum backing. Table 1 displays the variables and parameters used in the welding process. The joints were elaborated using the tool position control mode, with the axial force of 18 kN, to +0.5 mm offset, and 22 kN for +1.0 and +1.5 mm.

Microstructural characterization was performed using optical microscopy (OM) and scanning electron microscopy (FE-SEM). The samples were prepared using sandpaper from 100 to 1500 mesh, followed by polishing with 1.0 µm diamond paste. In order to observe the microstructure, the samples were etched with 2% nital, followed by etching with 1% hydrofluoric acid. The characterization of the steel particles was performed using the ImageJ software.

3. RESULTS

3. 1. Base Metal Figure 2 presents the microstructure of the metals used. For both the AISI-SAE 1020 and the AA6063 the structure is composed of equiaxial grains in all directions. In the steel workpiece (Figure 2a), the structure is formed by ferrite grains with

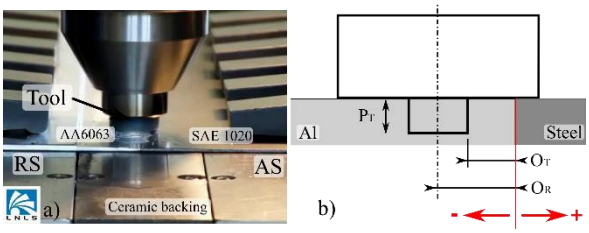

Figure 1. a) Photograph of the joint configuration, the tool and the backing. b) The positioning of the tool for determining the real (O_R) and tangent (O_T) offset. The red arrows and the positive and negative signs indicate the tool's position to the joint line. RS and AS corresponds to the retreating and advancing side, respectively

TABLE 1. Welding parameters for AA 6063-steel 1020 joints, to welding in different stages.

Test	ω (rpm)	υ (mm/min)	O_r (mm)	O_T (mm)	P_T (mm)
Ceramic backing	300	150	-2.1;-1.6;-1.1	0.5; 1.0; +1.5	1.65
Al backing	300	150	-3.1 to -0.6	-0.5 to +2.0	1.50 to 1.70

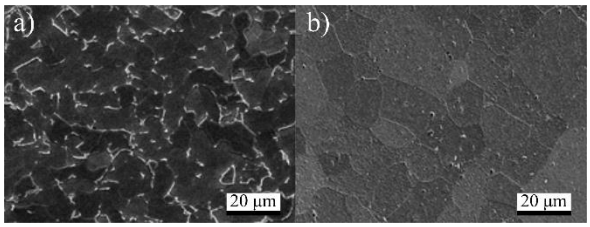

Figure 2. FE-SEM images showing the microstructure of a) AISI-SAE 1020 steel and b) AA6063-T5. Etching with nital for steel and hydrofluoric acid for aluminium

perlite (white). For the aluminum alloy (Figure 2b), the arrangement is of αAl grains, with the presence of β_{AlFeSi} particles, many of them dissolved (holes) by the action of the etchant [32]. In both cases, there is no evidence of the metal rolling process.

3. 2. Macrostructure, Production, and Control of Steel Particles Figure 3 shows the macrographs of the welded joints with O_T of +0.5 and +1.5. Two regions are easily identified on the aluminum side: nugget or stir zone (SZ), and the thermo-mechanically affected zone (TMAZ), while on the steel side, only TMAZ is evident. The welding parameters and the heat input control were essential in obtaining joints with a suitable surface appearance with no defects [33].

A similar structure, with a clear difference between the welded metals, was observed in dissimilar joints of AA7075-AA2024. The authors claim that low rotational speed negatively affects the joint, leading to absence of mixing. In contrast, satisfactory mixture is reached at high rotational speed. [34, 35]. It is not the case for aluminum-steel joints, where mixing does not occur in any condition, as highlighted by other authors [36, 37], who points out a clear limit between aluminum and steel. The only mixing occurs in the SZ, where steel fragments are observed, typical of this type of welded joint [38], [39].

The general appearance of the particles can be seen in Figure 4a. It would be plausible to believe that particles could come from the tool, but that possibility is completely ruled out. The fragments retain traces of the TMAZ, from where they were detached. For example, the cementite sheets are completely stretched by the high deformation of steel at the interface, in addition to the ferrite micro-grains formed by the dynamic recrystallization of the steel (Figure 4b). It also highlights the absence of intermetallic compounds (IMC) due to the absence of these deleterious phases in the welded joints, as it was indicated in previous work [40]. The absence of IMC contrasts those with other studies [41, 42], where these composites outline the particles, identified by Pourali et al. [43] as $FeAl_3$.

Lee et al. [44] attribute the formation of debris to the O_T's action, which leads to broken steel particles on the

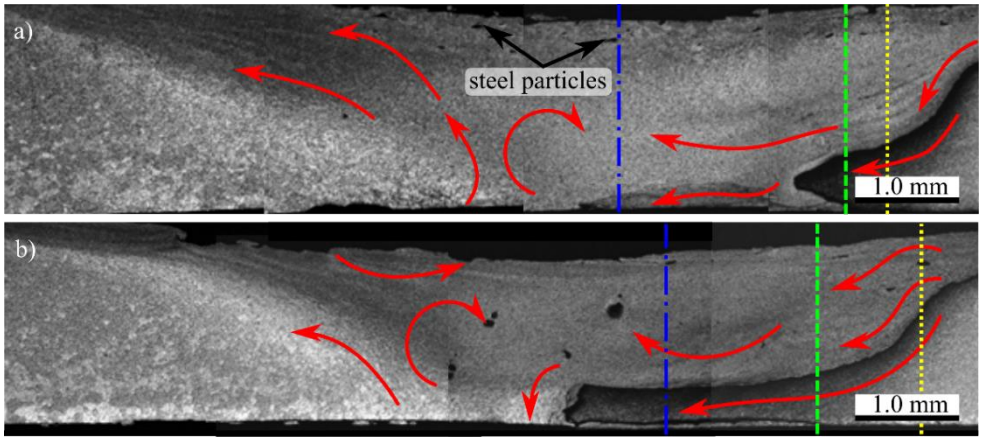

Figure 3. Macrograph of the welded joint's cross-section with O_T of a) +0.5, and b) +1.5 mm. The green, blue, and yellow lines correspond to the joint's original line, the tool axis, and the O_T, respectively. Red arrows indicate the direction of material flow

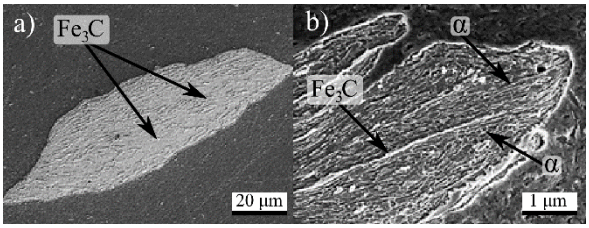

Figure 4. FE-SEM images of the particles observed in the SZ: a) big particle (180 µm) and b) detail showing the stretched lamellae of cementite and ferrite's nano-grains (α).

surface of welded joints being distributed within the SZ. Figure 5 shows images from top to bottom in joints with +0.5 and +1.5 mm offset. These images confirm the accumulation of the fragments, mainly on the surface, so it is defined that this is the most important place for its quantification.

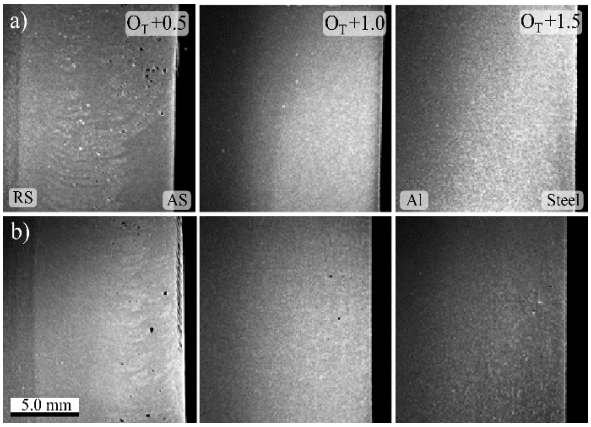

Figure 5. Distribution of steel fragments in the SZ in welded joints with offset a) +0.5 and b) +1.5 mm. The images were obtained with polished from the top at 0.5, 1.0, and 1.5 mm depth of the joint surface

The hypothesis that the quantity and size of the particles change with the O_T is being corroborated in Figure 6. Surprisingly, there is a constant reduction in the number of particles as the offset increases; the expected behavior was the opposite. Higher O_T means more interaction between tool and steel, which would easily explain the increased particle formation [45].

On the other hand, related to the steel particles size, Figure 6 does not show a discernible relationship with the offset, since it was expected that a higher O_T would generate large steel debris [46]. Figure 7 shows a more precise relation between offset and particle size by the distribution of the particle area. It confirms the reduction in the number of particles with O_T; besides, the figure registers that the particle size is less than 0.1 mm^2, for all conditions evaluated. Finally, the analysis leaves in mind that the particle size decreases with O_T, evidenced by the smaller number of particles larger than 1.0 mm^2, which confirms the reduction of both quantity and size with the offset.

Part of the formation and the detachment of the fragments are related to the generation of protuberances (Figure 8a). The tool shear stress promoted by plasticized aluminum entrance in small openings in the Al-steel

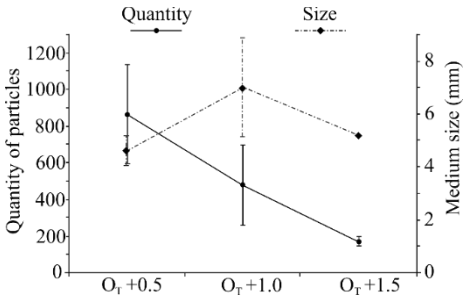

Figure 6. Effect of offset on the quantity and size of steel particles in the SZ.

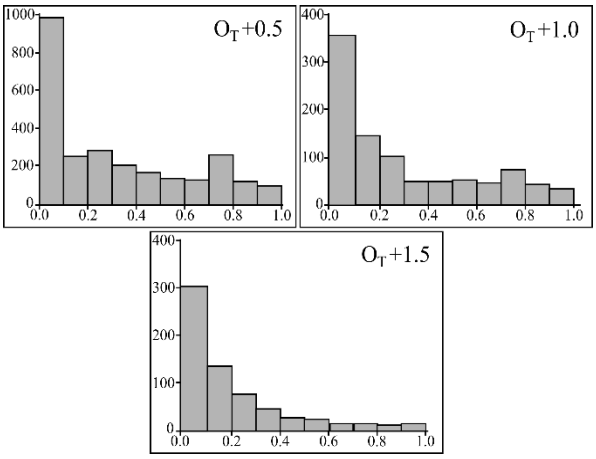

Figure 7. Measurement of the quantity and area of the steel fragments at the top of the SZ

interface (Figure 8b). Coelho et al. [47] observed the formation of similar structures that they defined as a non-smooth interface, to which the mechanical interlocking between both materials is attributed. Movahedi et al. [48] indicate that aluminum's entry favors IMC formation in a swirl-layer, formed by the mechanical mixture and the diffusion between aluminum and steel. However, this is not the case for the joints under study, as the phase in the openings corresponds completely to Al (Figure 8c).

In the flatter regions of the interface, the detachment mechanism is different, as it inVolves tearing the interface, as shown in Figure 9a, which leads to the removal of irregularities. The deformation at the interface is so high that it causes stretching and recrystallization of the ferrite grains; features are observed outside the steel fragments, as shown in Figure 9b.

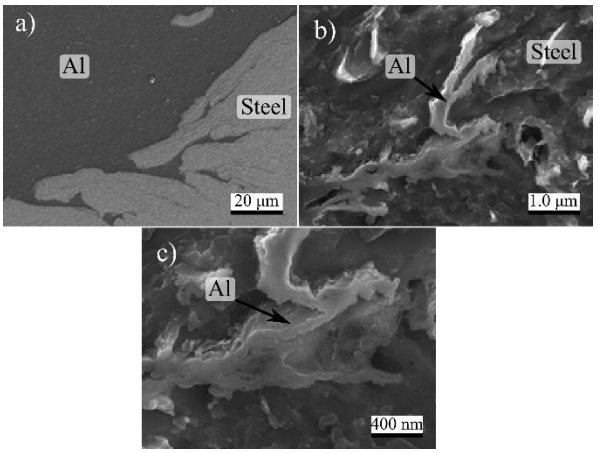

Figure 8. FE-SEM images of the final joint welded with a +1.5 mm offset. a) Formation of protuberances at the interface, b) ingress of aluminum into the steel, and c) cracking and separation of the protuberance

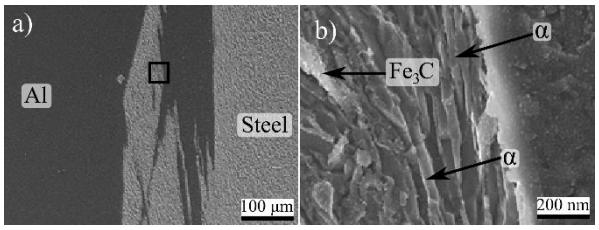

Figure 9. FE-SEM images of a) steel particle coming off the Al-steel interface and b) detail of the particle interface showing the severe deformation of the ferrite grains

3. 3. Metal Flow Figure 3 exposes the flow of material in the thin sheet Al-steel joint. Metal flow was described, considering morphological features observed in the macrographs such as banding, steel's profile at the interface, the shape of the SZ, and the steel fragments location. Kimapong and Watanabe [49] indicate that the particles aligned with the aluminum flow, as observed in Figure 10, follow the plasticized metal movement.

Banding is one of the most prominent peculiarities in the SZ of metals processed by FSW. In this process, the plasticized metal displacement occurs both in a laminar and vertical way. As the tool advances, plasticized metal is added layer-by-layer to the joint's back, which generates the banding, better known as the onion ring structure [50]. For the joints in question, this is more noticeable in regions with a considerable accumulation of

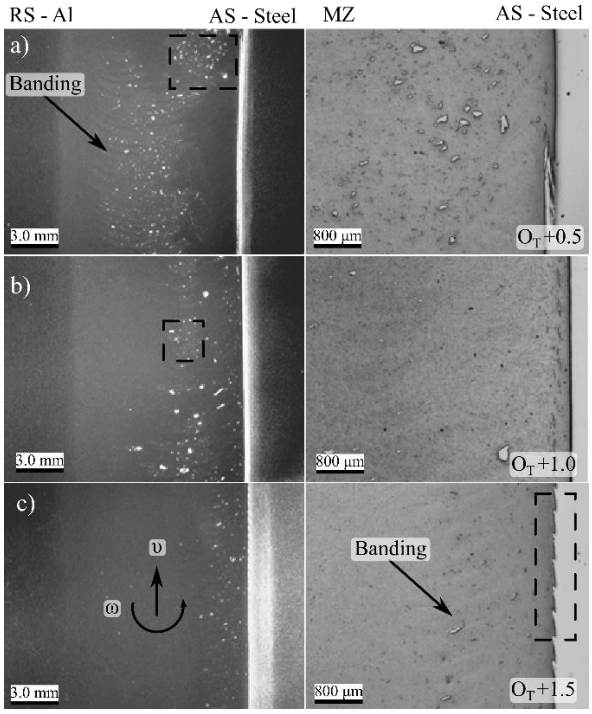

Figure 10. Macrographs at the top of the joints with an offset of a) +0.5; b) +1.0 and c) +1.5 mm.

steel fragments. Fonda and Bingert [51] established that these bands correspond to structural variations such as grain size, particle distribution, or texture, while multiple authors [52-55] report that the spacing between bands (λ) corresponds to the advance per reVolution (υ/ω).

Another critical point is the position of the particles. As presented in Figure 10, as the O_T increases, the steel fragments accumulate on the advanced side. This phenomenon can be justified considering the scheme of Figure 11a. Chen et al. [56] explain that the so-called shear zone occurs at the front of the pin, gradually growing as it moves towards the RS. The material transferred from the AS is moved towards the pin's back, generating a layer, which forms the banding. The highly deformed material flows around the pin forming the swirl zones. It is responsible for forming of defects such as voids when the plasticized metal's speed is lower to reach the metal at the rear of the advanced side [57]. Kumar and Kailas [58] point out that void defects are eliminated as welding forces increase, as the metal's extrusion force increases. However, other authors indicate that voids presence is the result of the lack of adherence between the plasticized metal and the pin [59, 60]. Kumar and Kailas [61] showed that for small O_T, much of the entrained material is deposited at the rear of the advanced side, which explains the position of the steel particles.

In a joint of the same material, the interaction between the tool and the pieces generates different forces represented in Figure 11b. Two types of forces can be highlighted: the normal force (F_n), generated by the forward movement of the tool, and the shear force (F_s) produced by the friction between the pin and the metal, where their direction and magnitude vary with the tool's position. Coelho et al. [62] agree with this approach but explain that they are two fundamental forces: the advanced force (F_{travel}) and the rotational force ($F_{rotation}$). Such forces are added or subtracted at some point, generating F_n and F_s; thus, the forces magnitude depends on the welding parameters and the welded metal's mechanical and physical properties.

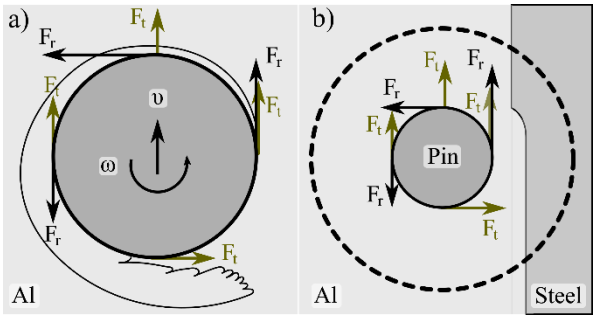

Figure 11. a) Diagram of the material flow in the shear zone around the pin (adapted from Chen et al. [56]). b) Diagram of the forces acting on the tool (adapted from Coelho et al. [62]).

Therefore, the shear force on the feed side ($F_{s(adv)}$) is the sum of F_{travel} and $F_{rotation}$, which generates a region of high forging pressure, accentuated by the constriction of the shoulder and the steel. This force is high enough to promote the steel's significant deformation and generate its recrystallization at the interface (Figure 9). When the force is very high, this leads to the stirring pin into the steel surface, producing the so-called fin-like shaper [63] observed in the rectangle in Figure 10c. This pressure on the advanced side pushes the steel down. However, the ceramic backing reacts against this movement, forcing the metal to move horizontally, below the pin, towards the aluminum side (Figure 3).

The deformation of the steel is different in the case of an aluminum backing. Figure 12 presents the welded joints results with the backing of AA5052, which shows the metal's full flow, without the restriction imposed by a higher hardness backing. This figure reveals how the steel moves and goes beyond the pin from the advanced to the retreating side. The effective depth (P_E) increases with the offset in joints welded with the same tool penetration (P_T). The flow of metal pushes the steel to the bottom from the AS, subsequently carried upwards when it reaches the RS. In this case, the upward movement of material is caused by the advanced side's metal flow.

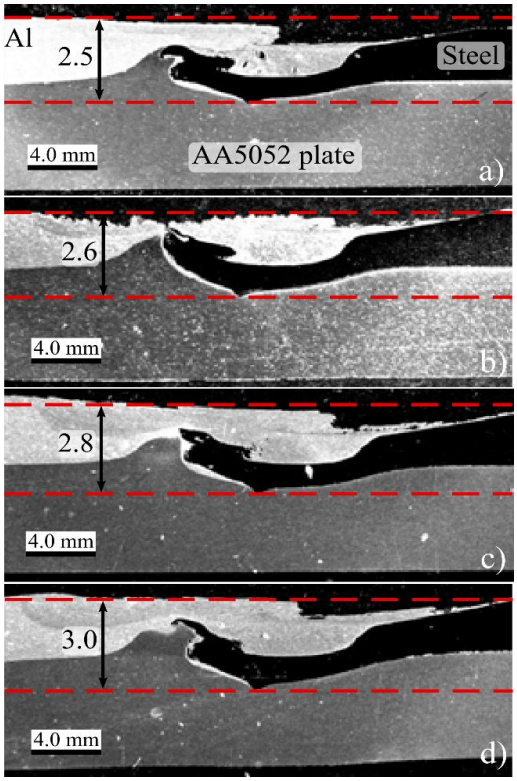

Figure 12. Pictures of FSW's aluminum-steel joint, using P_T 1.8 mm, O_T -0.3, +0.5, +1.3, and +2.0 mm, and AA5052 backing plate. The distance between the dashed lines (red) corresponds to the weld's P_E (in mm)

The upward movement of the steel on the RS (Figure 12) is the same that pushes the aluminum upward, on the same side at Al-steel joints (Figure 3). On this side, F_s is lower, since the advanced movement of the tool is opposite to the rotation, generating a low-pressure area, which favors the flow from the bottom to the surface.

4. DISCUSSION

The welding zone's morphological features are inherent to metal's flow, both in solid and plasticized state. One of the models in FSW considers the material flow as the sum of three combined movements: 1) a cylindrical flow around the pin, 2) a homogeneous flow parallels to the welding direction, and 3) an upward vortex-shaped flow around the pin [64]. Fonda et al. [65] explain that the flow around the pin is produced by the tool's rotation, which results in the shear deformation that originates from the shear zone. Likewise, they point out that the downward and upward movement of metal (vortex) is due to the threads and the tool's translation, generating the "onion ring". The spacing between bands corresponds to the tool advance per reVolution. Gerlich et al. [66] e Avettand-Fènoël et al. [67] also consider that the SZ was made up of only two flows: 1) the flow generated by the pin and 2) that produced by the axial force and rotation of the shoulder [50]. However, these theories are devised for the flow of metal in joints of the same metal. A few works make proposals for dissimilar joints between a soft metal and another of high resistance. Nevertheless, these elements must be considered to explain the observed behavior about the shape, distribution of steel particles in the SZ, and propose a model for FSW in thin Al-steel joints.

During the initial contact of the tool with the joint, the steel particles detachment occurs due to the shoulder's erosive action. The high pressure and the displacement of the plasticized aluminum cause the deformation of the wedge-shaped steel (Figure 3b). Texier et al. [68] point out that the intensity or speed at which extrusion occurs depends on the material's relative position to the pin. Doude et al. [69] studied the combined effect of shoulder and pin movements, added to the restriction imposed by backing, on the generation of symmetric vortex flow in the SZ (Figure 13a). However, in Al-steel joints, the symmetry is broken. The steel acts as another barrier to metal flow, altering the distribution of the plasticized material, allowing only its downward movement into the AS. In turn, this pushes the steel towards the bottom, to the pin's tip, and forces the steel to move horizontally in the direction of the RS (Figure 13b). The degree of deformation of the steel is subject to offset since this factor controls magnitude of the forging force. Wan and Huang [70] came to a similar result, where the forging force increased by the tool plunge.

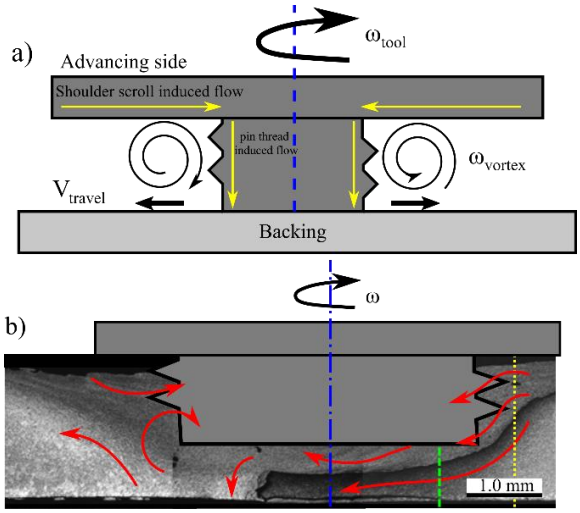

Figure 13. a) Scheme of the vortex generation in FSW in an aluminum joint and b) plot of the vortex and displacement of the metal in the Al-steel joint.

On the other hand, the steel particles detachment was produced by the interaction between the shoulder and the pushing force of plasticized metal removing irregularities from the steel surface, leaving it smoother. The shear movement generated by the pin promotes the emergence of irregularities and openings in the interface. However, as the offset increases, the forging pressure between the pin-shoulder and the steel is high enough to flatten the surface, reducing the number of irregularities and the detached particles mass. For this, the forging pressure close to the possible openings in the Al-steel interface, preventing the entrance of the plasticized metal. Smaller fragments come off since the irregularities are also smaller.

Most of the particles were formed by the contact between the shoulder and the joint surface. Few particles are dragged downwards, as shown by the series of images in Figure 5. Particles displaced by shoulder remain in their influences the area, while those caused inside the SZ are displaced to the surface by vortex movement. From this, it is essential to establish a link between the offset and the particles' position.

Liechty and Webb [71] determined flow lines in FSW, the result of which is superimposed on the macrographs of the deposits, as presented in Figure 14. A fraction of the pin interacts with the steel with a small offset, but such coincides with the flow that rotates more than 180° around the pin, allowing the fragments to pass from the AS to the RS and continue to the rear of the pin (Figure 14a). As O_T increases, many of the AS flow lines move parallel to the weld axis so that the detached particles are not trapped by the pin flow, crossing by the same AS (Figure 14b-c).

In another proposal for metal flow, Zeng et al. [72] relate the displacement of the plasticized metal with the

joint's temperature since it defines the degree of fluidity of the metal. Figures 14a-c shows Zeng's results superimposed with the particle distribution to +0.5, and +1.5 mm offset. For this type of joints, it was determined that both heat input and maximum temperature increase with the offset [73, 74], and in that sense, there is an agreement with Zang's proposal and the observed results.

In FSW, heat is the main product of friction between the shoulder and the joint [75], the shear deformation produced by the pin [76]. Therefore, the heat generation depends on contact conditions of the elements since the metal can stick or slide on the tool [77]. Idagawa et al. [78] relate the slip/stick conditions with the offset and the heat generation in these joints, through the slip/stick factor (δ) for each material (δ_{Al} and δ_{Steel}). If δ = 1, there is virtually no adherence between metal and tool, so the heat is generated mainly by friction.

On the other hand, if δ = 0, the heat is produced almost entirely by plastic deformation [79], [Souza et al. DOI: 10.3217/978-3-85125-615-4-33]]. Idagawa was able to establish that, on the aluminum side, the predominant mechanism for heat generation is plastic deformation, which implies that plasticized metal adheres to the tool, while for steel, the friction responds for 85% of the heat produced, consequently prevail slip on the steel-tool interaction. Even more important was to establish that δAl increases significantly with the offset, going from 0.02 to 0.40, meaning that adhesion is lost between the elements because the plasticized metal reaches significant fluidity. Therefore, this sings that the detached particles' location is related to the metal's fluidity, which depends on the joint's temperature, which in the case in question is subject to offset.

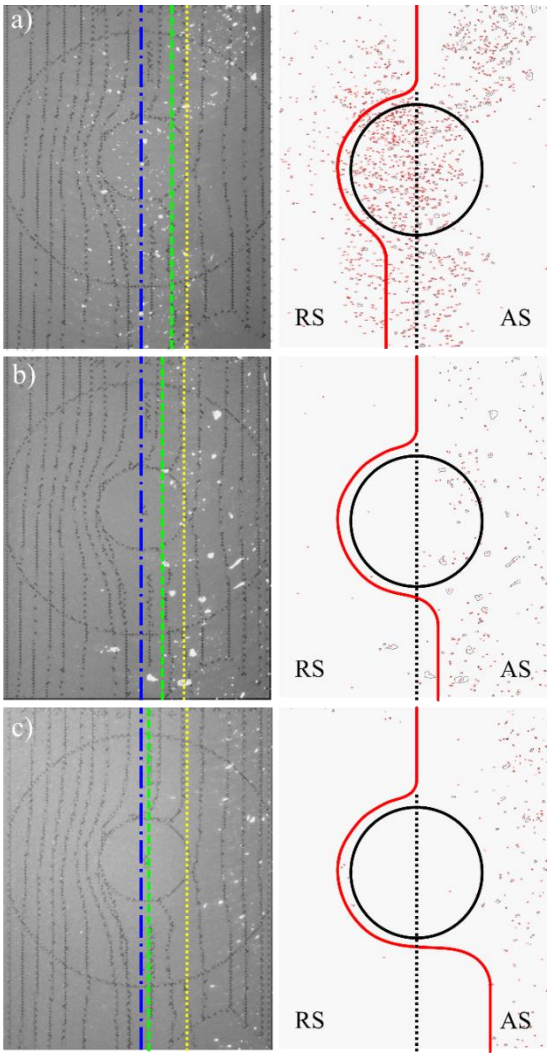

Figure 14. Overlapping between steel particle distribution and metal flow model proposed by Liechty and Webb [68], for offset: a) +0.5, b) +1.0, and c) +1.5 mm. Projection connecting the distribution of steel particles with the metal flow model proposed by Zeng et al. [69], for offset: a) +0.5, b) +1.0, and c) +1.5 mm. The green, blue, and yellow lines correspond to the original joint line, the tool axis, and the O_T, respectively

5. CONCLUSIONS

This work evaluated the generation and distribution of steel fragments and the metal flow in thin sheets of aluminum-steel welded joints. From the results and their analysis, the following points are concluded.

The detachment of steel particles was produced by two mechanisms: generation of protuberances at the interface by introducing plasticized aluminum and the tearing of the surface by the shear stress of the aluminum flow.

Detached particles correspond only to steel since they have cementite sheets and ultra-fine grains of ferrite, generated by the steel's high deformation and dynamic recrystallization.

The quantity of fragments decreases with the offset due to the reduction in protuberances formation by increasing the forging force, which inhibits plasticized aluminum entrance at the interface.

Forging force at AS increases with the offset, which implies that the steel's surface moves down and below the pin, where the restriction of the backing forces its horizontal displacement towards the RS.

The particles position is defined by the offset, which controls the plasticized fluidity of metals by determining the temperature in the joint. Large offset generates higher temperature and metal fluidity, allowing that particles to be dragged to the pin's back, closer to AS's interface. Meanwhile, a small offset decreases the temperature and fluidity of aluminums, promoting that the fragments are led to the pin's back, closer to the centerline.

The containment between the shoulder, pin, and backing, on the retreating side, promote the material to flow in a vortex shape. In contrast, on the advancing side,

the flow's symmetry is broken by the restriction imposed by the steel, which promotes shear and downward movement of the plasticized metal.

6. REFERENCES

1 S. Sheikhi and J. F. Dos Santos, "Effect of process parameter on mechanical properties of friction stir welded tailored blanks from aluminium alloy 6181-T4," ***Science and Technology of Welding and Joining***, Vol. 12, No. 4, 370-375, (2007), doi: 10.1179/174329307X173698.

2 K. Colligan, P. Konkol, J. Fisher, and J. Pickens, "Improved tools and process parameters were used to fabricate structures of 2519 aluminum armor for the U.S. Marine Corps' Advanced Amphibious Assault Vehicle," ***Welding Journal***, Vol. 82, No. 3, (2003).

3 M. Posada, J. P. Nguyen, D. R. Forrest, J. J. DeLoach, and R. Denale, "Friction stir welding advances joining technology," ***Amptiac Q.***, Vol. 7, No. 3, 13-20, (2003).

4 K. Colligan, "Friction stir welding for ship construction," ***Concurrent Technologies Corporation, Harrisburg, PA***. 2004, [Online]. Available: http://147.160.99.83/useruploads/file/publications/FSWShipConstruction.pdf.

5 S. W. Williams, "Welding of airframes using friction stir," Air Sp. Eur., Vol. 3, No. 3-4, 64-66, (2001), doi: 10.1016/s1290-0958(01)90059-0.

6 M. J. Brooker, A. J. M. Van Deudekom, S. W. Kallee, and P. D. Sketchley, "Applying friction stir welding to the Ariane 5 main motor thrust frame," European Space Agency, (Special Publication) ESA SP, No. 468. 507-511, (2001).

7 J. Ding, R. Carter, K. LA WLESS, A. Nunes, and C. Russell, "Friction stir welding flies high at NASA," ***Welding Journal***, Vol. 85, No. 3, 54-59, (2006).

8 W. M. Thomas, E. D. Nicholas, J. C. Needhan, M. G. Murch, P. Temple-Smith, and C. J. Dawes, "International patent application PCT/GB92/02203 and GB patent application 9125978.8," UK Patent Office, London. 1991.

9 R. S. Mishra and Z. Y. Ma, "Friction stir welding and processing," ***Materials Science and Engineering R: Reports,*** Vol. 50, No. 1-2. Elsevier, 1-78, (2005), doi: 10.1016/j.mser.2005.07.001.

10 I. T. C. ; J. Langari, F. Kolahan, and K. Aliakbari, "Effect of Tool Speed on Axial Force, Mechanical Properties and Weld Morphology of Friction Stir Welded Joints of A7075-T651," ***International Journal of Engineering, Transactions C: Aspects***, Vol. 29, No. 3, 403-410, (2016), doi: 10.5829/idosi.ije.2016.29.03c.15.

11 J. Q. Su, T. W. Nelson, R. Mishra, and M. Mahoney, "Microstructural investigation of friction stir welded 7050-T651 aluminium," ***Acta Materialia***, Vol. 51, No. 3, 713-729, (2003), doi: 10.1016/S1359-6454(02)00449-4.

12 R. Singh, S. A. Rizvi, and S. P. Tewari, "Effect of Friction Stir Welding on the Tensile Properties of AA6063 under Different Conditions," ***International Journal of Engineering, Transactions A: Basics***, Vol. 30, No. 4, 597-603, (2017).

13 R. M. Leal, C. Leitão, A. Loureiro, D. M. Rodrigues, and P. Vilaça, "Material flow in heterogeneous friction stir welding of thin aluminium sheets: Effect of shoulder geometry," ***Materials Science and Engineering A,*** Vol. 498, No. 1-2, 384-391, 2008, doi: 10.1016/j.msea.2008.08.018.

14 P. B. Prangnell and C. P. Heason, "Grain structure formation during friction stir welding observed by the 'stop action technique,'" ***Acta Materialia***, Vol. 53, No. 11, 3179-3192, (2005), doi: 10.1016/j.actamat.2005.03.044.

15 I. Transactions B ; J. Fabregas, A. Villegas, and J. Martínez Guarín, "A Coupled Rigid-viscoplastic Numerical Modeling for Evaluating Effects of Shoulder Geometry on Friction Stir-welded Aluminum Alloys," ***International Journal of Engineering, Transactions B: Applications,*** Vol. 32, No. 2, 313-321, (2019), doi: 10.5829/ije.2019.32.02b.17.

16 S. Xu and X. Deng, "A study of texture patterns in friction stir welds," ***Acta Materialia***, Vol. 56, No. 6, 1326-1341, 2008, doi: 10.1016/j.actamat.2007.11.016.

17 O. D. Hincapié, J. A. Salazar, J. J. Restrepo, E. A. Torres, and J. Graciano-Uribe, "Control of Formation of Intermetallic Compound in Dissimilar Joints Aluminum-steel," ***International Journal of Engineering, Transactions A: Basics***, Vol. 32, No. 1, 127-136, (2019), Accessed: Jul. 13, 2019. [Online].

18 N. Ethiraj, T. Sivabalan, B. Sivakumar, S. Vignesh Amar, N. Vengadeswaran, and K. Vetrivel, "Effect of tool rotational speed on the tensile and microstructural properties of friction stir welded different grades of stainless steel joints," ." ***International Journal of Engineering, Transactions A: Basics***, Vol. 33, No. 1, 141-147, (2020), doi: 10.5829/ije.2020.33.01a.16.

19 L. E. Murr, "A review of FSW research on dissimilar metal and alloy systems," ***Journal of Materials Engineering and Performance***, Vol. 19, No. 8, 1071-1089, (2010), doi: 10.1007/s11665-010-9598-0.

20 T. DebRoy and H. K. D. H. Bhadeshia, "Friction stir welding of dissimilar alloys - A perspective," ***Science and Technology of Welding and Joining***, Vol. 15, No. 4, 266-270, (2010), doi: 10.1179/174329310X12726496072400.

21 V. Firouzdor and S. Kou, "Al-to-Mg friction stir welding: Effect of material position, travel speed, and rotation speed," ***Metallurgical and Materials Transactions A Physical Metallurgy and Materials Science***, Vol. 41, No. 11, 2914-2935, (2010), doi: 10.1007/s11661-010-0340-1.

22 T. Kakiuchi, Y. Uematsu, and K. Suzuki, "Evaluation of fatigue crack propagation in dissimilar Al/steel friction stir welds," **in** ***Procedia Structural Integrity***, (2016), Vol. 2, 1007-1014, doi: 10.1016/j.prostr.2016.06.129.

23 S. Y. Anaman, H. H. Cho, H. Das, J. S. Lee, and S. T. Hong, "Microstructure and mechanical/electrochemical properties of friction stir butt welded joint of dissimilar aluminum and steel alloys," ***Materials Characterization***, Vol. 154, 67-79, (2019), doi: 10.1016/j.matchar.2019.05.041.

24 T. Yasui, T. Ishii, Y. Shimoda, M. Tsubaki, M. Fukumoto, and T. Shinoda, "Friction stir welding between aluminum and steel with high welding speed," ***Production.*** 2004.

25 Q. Zheng, X. Feng, Y. Shen, G. Huang, and P. Zhao, "Dissimilar friction stir welding of 6061 Al to 316 stainless steel using Zn as a filler metal," ***Journal of Alloys and Compounds***, Vol. 686, 693-701, (2016), doi: 10.1016/j.jallcom.2016.06.092.

26 T. Wang, H. Sidhar, R. S. Mishra, Y. Hovanski, P. Upadhyay, and B. Carlson, "Evaluation of intermetallic compound layer at aluminum/steel interface joined by friction stir scribe technology," ***Materials and Design,*** Vol. 174, 107795, (2019), doi: 10.1016/j.matdes.2019.107795.

27 B. Seo, K. H. Song, and K. Park, "Corrosion Properties of Dissimilar Friction Stir Welded 6061 Aluminum and HT590 Steel," ***Metals and Materials International,*** Vol. 24, No. 6, 1232-1240, (2018), doi: 10.1007/s12540-018-0135-2.

28 M. Thomä, G. Wagner, B. Straß, B. Wolter, S. Benfer, and W. Fürbeth, "Ultrasound enhanced friction stir welding of aluminum and steel: Process and properties of EN AW 6061/DC04-Joints," ***Journal of Materials Science and Technology***, Vol. 34, No. 1, 163-172, (2018), doi: 10.1016/j.jmst.2017.10.022.

29 Y. Huang *et al.*, "Material-flow behavior during friction-stir welding of 6082-T6 aluminum alloy," ***The International Journal of Advanced Manufacturing Technology***, Vol. 87, No. 1-4,

1115-1123, (2016), doi: 10.1007/s00170-016-8603-7.

30 K. Colligan, "Material flow behavior during friction stir welding of aluminum," ***Weld. Journal-New York***-, Vol. 78, 229-s, 1999.

31 T. F. A. Santos, E. A. Torres, T. F. C. Hermengildo, and A. J. Ramirez, "Development of ceramic backing for friction stir welding and processing," ***Welding International***, Vol. 30, No. 5, 338-347, (2016), doi: 10.1080/09507116.2015.1096498.

32 E. Torres and A. Ramirez, "União de juntas dissimilares alumínio-aço de chapas finas pelo processo de soldagem por atrito com pino não consumível (sapnc)," Soldag. e Insp., Vol. 16, No. 3, 265-273, (2011), doi: 10.1590/S0104-92242011000300008.

33 E. Torres and A. Ramirez, "Efeito dos parâmetros de processo na obtenção e na microestrutura de juntas alumínio-aço realizadas mediante Soldagem POR Atrito COM Pino nãO Consumível (SAPNC)," Soldag. e Insp., Vol. 18, No. 3, 245-256, (2013), doi: 10.1590/S0104-92242013000300007.

34 P. Alvarez, G. Janeiro, A. A. M. Da Silva, E. Aldanondo, and A. Echeverría, "Material flow and mixing patterns during dissimilar FSW," in ***Science and Technology of Welding and Joining***, (2010), Vol. 15, No. 8, 648-653, doi: 10.1179/136217110X12785889549543.

35 A. A. M. da Silva, E. Arruti, G. Janeiro, E. Aldanondo, P. Alvarez, and A. Echeverria, "Material flow and mechanical behaviour of dissimilar AA2024-T3 and AA7075-T6 aluminium alloys friction stir welds," ***Materials and Design***, Vol. 32, No. 4, 2021-2027, (2011), doi: 10.1016/j.matdes.2010.11.059.

36 W. H. Jiang and R. Kovacevic, "Feasibility study of friction stir welding of 6061-T6 aluminium alloy with AISI 1018 steel," *Proc. **Inst. Mech. Eng. Part B J. Eng. Manuf***., Vol. 218, No. 10, 1323-1331, 2004, doi: 10.1243/0954405042323612.

37 H. Uzun, C. Dalle Donne, A. Argagnotto, T. Ghidini, and C. Gambaro, "Friction stir welding of dissimilar Al 6013-T4 To X5CrNi18-10 stainless steel," ***Materials and Design***, Vol. 26, No. 1, 41-46, (2005), doi: 10.1016/j.matdes.2004.04.002.

38 S. Amini and M. R. Amiri, "Study of ultrasonic vibrations' effect on friction stir welding," ***The International Journal of Advanced Manufacturing Technology***, Vol. 73, No. 1-4, 127-135, 2014, doi: 10.1007/s00170-014-5806-7.

39 R. Rafiei, A. Ostovari Moghaddam, M. R. Hatami, F. Khodabakhshi, A. Abdolahzadeh, and A. Shokuhfar, "Microstructural characteristics and mechanical properties of the dissimilar friction-stir butt welds between an Al-Mg alloy and A316L stainless steel," ***The International Journal of Advanced Manufacturing Technology***, Vol. 90, No. 9-12, 2785-2801, (2017), doi: 10.1007/s00170-016-9597-x.

40 E. A. Torres López and A. J. Ramirez, "Inhibition of the formation of intermetallic compounds in aluminum-steel welded joints by friction stir welding," ***Revista de Metalurgia,*** Vol. 51, No. 4, 1-10, 2015, doi: 10.3989/revmetalm.053.

41 T. Chen, "Process parameters study on FSW joint of dissimilar metals for aluminum-steel," ***Journal* of Materials *Science***, Vol. 44, No. 10, 2573-2580, (2009), doi: 10.1007/s10853-009-3336-8.

42 X. Liu, S. Lan, and J. Ni, "Analysis of process parameters effects on friction stir welding of dissimilar aluminum alloy to advanced high strength steel," ***Materials and Design***, Vol. 59, 50-62, 2014, doi: 10.1016/j.matdes.2014.02.003.

43 M. Pourali, A. Abdollah-zadeh, T. Saeid, and F. Kargar, "Influence of welding parameters on intermetallic compounds formation in dissimilar steel/aluminum friction stir welds," ***J. Alloys Compd.***, Vol. 715, 1-8, (2017), doi: 10.1016/j.jallcom.2017.04.272.

44 W. B. Lee, M. Schmuecker, U. A. Mercardo, G. Biallas, and S. B. Jung, "Interfacial reaction in steel-aluminum joints made by friction stir welding," ***Scripta Materialia*** , Vol. 55, No. 4, 355-358, (2006), doi: 10.1016/j.scriptamat.2006.04.028.

45 A. A. Fallahi, A. Shokuhfar, A. Ostovari Moghaddam, and A. Abdolahzadeh, "Analysis of SiC nano-powder effects on friction stir welding of dissimilar Al-Mg alloy to A316L stainless steel," ***Journal of Manufacturing Processes***, Vol. 30, 418-430, (2017), doi: 10.1016/j.jmapro.2017.09.027.

46 X. Liu, S. Lan, and J. Ni, "Experimental investigation on joining dissimilar aluminum alloy 6061 to TRIP 780/800 steel through friction stir welding," ***Journal of Engineering Materials and Technology, Transactions of the ASME***, Vol. 137, No. 4, 2015, doi: 10.1115/1.4030480.

47 R. S. Coelho, A. Kostka, J. F. dos Santos, and A. Kaysser-Pyzalla, "Friction-stir dissimilar welding of aluminium alloy to high strength steels: Mechanical properties and their relation to microstructure," ***Materials Science and Engineering A*** , Vol. 556, 175-183, (2012), doi: 10.1016/j.msea.2012.06.076.

[48 M. Movahedi, A. H. Kokabi, S. M. Seyed Reihani, and H. Najafi, "Effect of tool travel and rotation speeds on weld zone defects and joint strength of aluminium steel lap joints made by friction stir welding," ***Science and Technology of Welding and Joining***, Vol. 17, No. 2, 162-167, (2012), doi: 10.1179/1362171811Y.0000000092.

49 K. Kimapong and T. Watanabe, "Friction stir welding of aluminum alloy to steel," ***Welding Journal***, Vol. 83, No. 10, p. 277, 2004.

50 F. Gratecap, M. Girard, S. Marya, and G. Racineux, "Exploring material flow in friction stir welding: Tool eccentricity and formation of banded structures," ***International Journal of Material Forming***, Vol. 5, No. 2, 99-107, (2012), doi: 10.1007/s12289-010-1008-5.

51 R. W. Fonda and J. F. Bingert, "Texture variations in an aluminum friction stir weld," ***Scripta Materialia*** , Vol. 57, No. 11, 1052-1055, (2007), doi: 10.1016/j.scriptamat.2007.06.068.

52 S. Muthukumaran and S. K. Mukherjee, "Multi-layered metal flow and formation of onion rings in friction stir welds," ***The International Journal of Advanced Manufacturing Technology***, Vol. 38, No. 1-2, 68-73, (2008).

53 Z. W. Chen and S. Cui, "On the forming mechanism of banded structures in aluminium alloy friction stir welds," ***Scripta Materialia ,*** Vol. 58, No. 5, 417-420, Mar. (2008), doi: 10.1016/j.scriptamat.2007.10.026.

54 J. Teimournezhad and A. Masoumi, "Experimental investigation of onion ring structure formation in friction stir butt welds of copper plates produced by non-threaded tool pin," ***Science and Technology of Welding and Joining***, Vol. 15, No. 2, 166-170, 2010, doi: 10.1179/136217109X12577814486610.

55 J. Schneider, S. Brooke, and A. C. Nunes, "Material Flow Modification in a FSW Through Introduction of Flats," ***Metall. Mater. Trans. B Process Metall. Mater. Process.*** *Sci.*, Vol. 47, No. 1, 720-730, (2016), doi: 10.1007/s11663-015-0523-7.

56 Z. W. Chen, T. Pasang, and Y. Qi, "Shear flow and formation of Nugget zone during friction stir welding of aluminium alloy 5083-O," ***Materials Science and Engineering A ,*** Vol. 474, No. 1-2, 312-316, (2008), doi: 10.1016/j.msea.2007.05.074.

57 A. Tongne, C. Desrayaud, M. Jahazi, and E. Feulvarch, "On material flow in Friction Stir Welded Al alloys," ***Journal of Materials Processing Technology***, Vol. 239, 284-296, (2017), doi: 10.1016/j.jmatprotec.2016.08.030.

58 K. Kumar and S. V. Kailas, "The role of friction stir welding tool on material flow and weld formation," ***Materials Science and Engineering A*** , Vol. 485, No. 1-2, 367-374, (2008), doi: 10.1016/j.msea.2007.08.013.

59 R. Zettler *et al.*, "Effect of tool geometry and process parameters on material flow in FSW of AN AA 2024-T351 alloy," in ***Welding in the World,*** (2005), Vol. 49, No. 3-4, 41-46, doi: 10.1007/BF03266474.

60 Y. H. Zhao, S. B. Lin, F. X. Qu, and L. Wu, "Influence of pin geometry on material flow in friction stir welding process," ***Materials Science and Technology*** , Vol. 22, No. 1, 45-50, (2006), doi: 10.1179/174328406X78424.

61 K. Kumar and S. V. Kailas, "Positional dependence of material flow in friction stir welding: Analysis of joint line remnant and its relevance to dissimilar metal welding," ***Science and Technology of Welding and Joining***, Vol. 15, No. 4, 305-311, (2010), doi: 10.1179/136217109X12568132624280.

62 R. S. Coelho, A. Kostka, J. dos Santos, and A. R. Pyzalla, "EBSD Technique Visualization of Material Flow in Aluminum to Steel Friction-stir Dissimilar Welding," ***Advanced Engineering Materials***, Vol. 10, No. 12, 1127-1133, (2008), doi: 10.1002/adem.200800227.

[63 K. Kimapong and T. Watanabe, "Lap Joint of A5083 Aluminum Alloy and SS400 Steel by Friction Stir Welding," ***Materials Transactions*** Vol. 46, No. 4, 835-841, (2005), doi: 10.2320/matertrans.46.835.

64 J. A. Schneider and A. C. Nunes, "Characterization of plastic flow and resulting microtextures in a friction stir weld," ***Metallurgical and Materials Transactions B Process Metallurgy and Materials Science***, Vol. 35, No. 4, 777-783, 2004, doi: 10.1007/s11663-004-0018-4.

65 R. Fonda, A. Reynolds, C. R. Feng, K. Knipling, and D. Rowenhorst, "Material flow in friction stir welds," ***Metallurgical and Materials Transactions A Physical Metallurgy and Materials Science***, Vol. 44, No. 1, 337-344, (2013), doi: 10.1007/s11661-012-1460-6.

66 A. Gerlich, P. Su, M. Yamamoto, and T. H. North, "Material flow and intermixing during dissimilar friction stir welding," ***Science and Technology of Welding and Joining***, Vol. 13, No. 3, 254-264, (2008), doi: 10.1179/174329308X283910.

67 M. N. Avettand-Fenoel, R. Taillard, J. Laye, and T. O. Vre, "Experimental investigation of three-dimensional (3-D) material flow pattern in thick dissimilar 2050 friction-stir welds," ***Metallurgical and Materials Transactions A Physical Metallurgy and Materials Science***, Vol. 45, No. 2, 563-578, 2014, doi: 10.1007/s11661-013-2015-1.

68 D. Texier, Y. Zedan, T. Amoros, E. Feulvarch, J. C. Stinville, and P. Bocher, "Near-surface mechanical heterogeneities in a dissimilar aluminum alloys friction stir welded joint," ***Materials and Design***, Vol. 108, 217-229, (2016), doi: 10.1016/j.matdes.2016.06.091.

69 H. R. Doude, J. A. Schneider, and A. C. Nunes, "Influence of the tool shoulder contact conditions on the material flow during friction stir welding," ***M Metallurgical and Materials Transactions A Physical Metallurgy and Materials Science***, Vol. 45, No. 10, 4411-4422, 2014, doi: 10.1007/s11661-014-2384-0.

70 L. Wan and Y. Huang, "Friction stir welding of dissimilar aluminum alloys and steels: a review," ***The International Journal of Advanced Manufacturing Technology***, Vol. 99, No. 5-8, 1781-1811, (2018), doi: 10.1007/s00170-018-2601-x.

71 B. C. Liechty and B. W. Webb, "Flow field characterization of friction stir processing using a particle-grid method," ***Journal of Materials Processing Technology***, Vol. 208, No. 1-3, 431-443, (2008), doi: 10.1016/j.jmatprotec.2008.01.008.

72 X. H. Zeng, P. Xue, D. Wang, D. R. Ni, B. L. Xiao, and Z. Y. Ma, "Effect of Processing Parameters on Plastic Flow and Defect Formation in Friction-Stir-Welded Aluminum Alloy," ***Metallurgical and Materials Transactions A Physical Metallurgy and Materials Science***, Vol. 49, No. 7, 2673-2683, (2018), doi: 10.1007/s11661-018-4615-2.

73 X. Liu, G. Chen, J. Ni, and Z. Feng, "Computational Fluid Dynamics Modeling on Steady-State Friction Stir Welding of Aluminum Alloy 6061 to TRIP Steel," ***Journal of Manufacturing Science and Engineering, Transactions of the ASME***, Vol. 139, No. 5, (2017), doi: 10.1115/1.4034895.

74 K. Chen, X. Liu, and J. Ni, "A review of friction stir-based processes for joining dissimilar materials," ***The International Journal of Advanced Manufacturing Technology***, Vol. 104, No. 5-8, 1709-1731, (2019), doi: 10.1007/s00170-019-03975-w.

75 Frigaard, Grong, and O. T. Midling, "A process model for friction stir welding of age hardening aluminum alloys," ***Metallurgical and Materials Transactions A Physical Metallurgy and Materials Science***, Vol. 32, No. 5, 1189-1200, (2001), doi: 10.1007/s11661-001-0128-4.

76 M. Z. H. Khandkar, J. A. Khan, and A. P. Reynolds, "Prediction of temperature distribution and thermal history during friction stir welding: input torque based model," ***Science and Technology of Welding and Joining***, Vol. 8, No. 3, 165-174, (2003).

77 J. Schneider, R. Beshears, and A. C. Nunes, "Interfacial sticking and slipping in the friction stir welding process," ***Materials Science and Engineering A*** , Vol. 435-436, 297-304, (2006), doi: 10.1016/j.msea.2006.07.082.

78 H. S. Idagawa, E. A. Torres, and A. J. Ramirez, "CFD modeling of dissimilar aluminum-steel friction stir welds," (2013).

79 R. Nandan, T. DebRoy, and H. K. D. H. Bhadeshia, "Recent advances in friction-stir welding - Process, weldment structure and properties," ***Progress in Materials Science***, Vol. 53, No. 6. Pergamon, 980-1023, (2008), doi: 10.1016/j.pmatsci.2008.05.001.

Persian Abstract

چکیده

در سی سال گذشته، فرآیند جوش‌کاری اصطکاکی اغتشاشی (FSW) به دلیل نتایج رضایت‌بخش حاصل از تغییر شکل شدید و گرمای کم ورودی در طول تولید اتصال جوش داده شده، اهمیت قابل توجهی یافته است. این عناصر برای پیاده سازی FSW در سیستم‌های جوش داده شده مختلف از جمله اتصالات آلومینیوم – فولاد در نظر گرفته شده‌اند. در این اتصالات غیرمشابه، هدف اصلی به دست آوردن یک اتصال جوش‌داده‌شده با رفتار مکانیکی قابل قبول بود. اخیراً برخی از مقاله‌ها بر درک فرآیند اتصالات غیرمشابه، عمدتا در جریان فلز و واکنش آن در برابر خوردگی متمرکز شده‌اند. با این حال، در اتصالات فولاد–آلومینیم، حضور ذرات فولاد در منطقه‌ی گرده‌ی جوش یک امر عادی است. این رفتار مکانیکی و شیمیایی اتصالات جوش داده شده را تغییر می‌دهد. بنابراین، هدف این پژوهش ارزیابی سازوکارهای تولید این ذرات و تعیین اثر انحراف ابزار در شکل گیری آنها و پیشنهاد رفتار جریان مواد با استفاده از ذرات جدا شده به عنوان ردیاب است. مشخص شد که انحراف ابزار سیالیت فلز را کنترل می کند، که به دلیل کاهش بی‌نظمی در رابط فولاد–آلومینیم امکان تجمع ذرات فولادی در سمت جلو و کاهش مقدار آن را فراهم می کند. به همین ترتیب، همان طور که در اتصالات آلومینیوم ذکر شده است، جریان فلز در سمت عقب مشاهده شد. در مقابل، در سمت جلو، یک حرکت برشی، فشار به سمت پایین و حرکت جانبی به سمت عقب، که توسط مقاومت نیروی آهنگری بالای فلز و محدودیت‌های اعمال شده توسط فولاد و ورق پشت‌بند حرکت می کند، وجود دارد.